Biodistribution and Radiation Dosimetry of the Dopamine Transporter Ligand [^{18}F]FECNT

Todd A. Deterding, John R. Votaw, Chris K. Wang, Dennis Eshima, Lori Eshima, Robert Keil, Eugene Malveaux, Clinton D. Kilts, Mark M. Goodman, and John M. Hoffman

Center for PET, Division of Nuclear Medicine, Department of Radiology, Emory University Hospital, Atlanta; and School of Mechanical Engineering, Georgia Institute of Technology, Atlanta, Georgia

^{18}F-labeled 2 β-carbomethoxy-3β-(4-chlorophenyl)-8-(−2-fluoroethyl)nortropane ([^{18}F]FECNT) is a recently developed dopamine transporter ligand with potential applications in patients with Parkinson's disease and cocaine addiction. **Methods:** Estimates of the effective dose equivalent and doses for specific organs were made using biodistribution data from 16 Sprague-Dawley rats and nine rhesus monkeys. PET images from two rhesus monkeys were used to calculate the residence time for the basal ganglia. The computer program MIRDOSE3 was used to calculate the dosimetry according to the methodology recommended by MIRD. **Results**: The basal ganglia were the targeted tissues receiving the highest dose, 0.11 mGy/MBq (0.39 rad/mCi). The effective dose equivalent was 0.018 mSv/MBq (0.065 rem/mCi), and the effective dose was 0.016 mSv/MBq (0.058 rem/mCi). **Conclusion:** Our data show that a 185-MBq (5-mCi) injection of [^{18}F]FECNT leads to an estimated effective dose of 3 mSv (0.3 rem) and an estimated dose to the target organ or tissue of 19.4 mGy (1.93 rad).

Key Words: dosimetry; dopamine transporter; [^{18}F]FECNT

J Nucl Med 2001; 42:376–381

The subjective and psychomotor stimulant effects of cocaine have been attributed to an inhibition of the reuptake of dopamine (DA) by its transporter (*1*,*2*). Also, a decrease in transporter density in the basal ganglia has been associated with Parkinson's disease (*3*). ^{18}F-labeled 2 β-carbomethoxy-3β-(4-chlorophenyl)-8-(−2-fluoroethyl)nortropane ([^{18}F]FECNT) is a DA transporter ligand recently developed for use in PET studies. [^{18}F]FECNT may possess the compartmental kinetic properties necessary to effectively study drug- or disease-related changes to transporters in the brain dopaminergic system (*4*,*5*). We present preliminary estimates of the absorbed dose from [^{18}F]FECNT.

Received May 16, 2000; revision accepted Sep. 29, 2000.

For correspondence or reprints contact: John R. Votaw, PhD, Department of Radiology, Emory University School of Medicine, 1364 Clifton Rd., NE, Atlanta, GA 30322.

MATERIALS AND METHODS

[^{18}F]FECNT

[^{18}F]FECNT was prepared by a two-step reaction sequence as previously described (*4*,*6*). Alkylation of 1-[^{18}F]fluoro-2-tosyloxyethane with 2β-carbomethoxy-3β-(4-chlorophenyl)nortropane in dimethyl formamide at 1,350°C for 45 min allowed [^{18}F]FECNT, which was purified by semipreparatory, reverse-phase high-performance liquid chromatography (HPLC), to produce a product free from the precursor, 2β-carbomethoxy-3β-(4-chlorophenyl)nortropane and with specific activity of 56 MBq/nmol (1.5 Ci/mmol).

Sprague-Dawley Rat Biodistribution Studies

Sixteen male Sprague-Dawley rats weighing between 250 and 300 g were anesthetized by an intramuscular injection of a 1:1 mixture of ketamine and xylazine. An incision was made to isolate and cannulate the femoral vein for administration of approximately 3.7 MBq (100 mCi) [^{18}F]FECNT in 0.25 mL 12% ethanol in saline as has been previously reported (*7*). Four animals each were killed at 5, 30, 60, and 120 min after injection and exsanguinated, and the brain, heart, lungs, liver, spleen, kidneys, and testes were rapidly removed. Additional samples of blood, muscle, and bone were also obtained. The radioactivity in these samples was assayed in an automated well counter (Cobra II Gamma automatic-counter Model 5002; Packard Instrument Co., Meriden, CT). All measurements were background subtracted and decay corrected to the time of killing, then averaged together. Uncertainties in the determinations were minimal, because each assay collected at least 10,000 counts. Uncertainties in dosimetry were determined from the estimated variation between samples as described below.

Rhesus Monkey Biodistribution Studies

Nine male rhesus monkeys, weighing an average of 5 kg, were first tranquilized with an intramuscular injection of Telazol (3 mg/kg), then anesthetized further by inhalation of isoflurane through a face mask, and next injected intravenously with [^{18}F]FECNT. Approximately 2 h elapsed before four of the monkeys were placed in the ECAT 951 PET scanner (Siemens, Hoffman Estates, IL) for a 30-min acquisition.

At the end of acquisition, the monkeys were removed from the scanner and immediately euthanized with barbiturates. Measurements of radioactivity in the liver, spleen, lung, testes, bone, kidney, skeletal muscle, heart wall, and selected regions of the brain, including the cerebellum and basal ganglia, were performed. For each of these measurements, two samples

were weighed and then counted in the automated well counter to determine the percentage of injected activity per gram, with all samples background subtracted and decay corrected to the time of killing, and then similar samples were averaged together.

Quantitative dynamic brain images were acquired from three rhesus monkeys (Fig. 1). The monkeys were anesthetized as previously described, and a femoral arterial catheter was inserted to obtain blood samples. A slow bolus injection of [^{18}F]FECNT over 30 s coincided with the start of the acquisition. Dynamic emission data were acquired using a 2-h, 18-image acquisition protocol. These three monkeys were then killed, and an identical study of organ distribution of radioactivity was performed as previously described. The kill times for the seven monkeys ranged from 174 to 352 min after injection.

The final two monkeys were studied with [^{18}F]FECNT using a 4-h, 32-image dynamic acquisition protocol after a slow 5-min, 1 mL/min infusion of 160 MBq (4.31 mCi) and 230 MBq (6.2 mCi) of the tracer. Regions of interest (ROIs) were drawn over the putamen, cerebellum, and whole brain. Time–activity curves (TACs) from these regions were used to calculate the residence time of [^{18}F]FECNT in the brain and basal ganglia as described below.

Residence Time Calculations

The TACs used to compute the residence times necessary in the MIRD method were extrapolated from the biodistribution data collected at different kill times from the Sprague-Dawley rats and rhesus monkeys. The rhesus monkey biodistribution data (percentage uptake of injected activity per gram of sample organ) for the blood, heart, lungs, liver, spleen, kidneys, bone, muscle, and testis at each kill time were multiplied by the reference man organ mass to reflect the percentage injected dose per organ in reference man (*8*,*9*).

The rat biodistribution data were used to better estimate the shape of the early part of the TAC. Because we assumed that the rhesus data would be better for estimating uptake in humans, the rat data were scaled to match the monkey data at 150 min after injection. The combined data were then used to calculate the residence time. After the last killing time (t = 352 min), the activity for each organ studied was assumed to leave by the clearance rate estimated from a monoexponential curve fit to the monkey data. The more conservative assumption that, after the last time point, all radioactivity leaves by natural decay alone would have been too conservative for organs with rapid clearance, such as the brain and lungs. The residence time for all unaccounted activity was assigned to the total body. Computation of the organ residence times used trapezoidal integration of the TAC plus analytic integration of the fit curve (after 352 min). Table 1 and Figure 2 illustrate these steps in calculations for the testis.

The TACs for the entire brain were determined by calculating the average pixel value in a multiplane ROI encompassing the entire brain of the two monkeys studied with the 4-h dynamic image acquisitions. The uptake associated with the basal ganglia was subtracted from the whole-brain TACs to obtain the non–basal ganglia–, non–dopamine transporter–related uptake of [^{18}F]FECNT in the brain.

Estimation of the radiation absorbed dose to a human was then calculated by entering the residence times for the brain, heart contents, cortical and trabecular bone, heart wall, kidneys, liver, lungs, muscle, spleen, testis, and total body into the MIRDOSE3 computer program (*10*) for a 70-kg adult male phantom. For a conservative estimation, the residence time for activity in the bone was considered evenly split between cortical and trabecular bone and was treated as if it were distributed on the bone surfaces. The heart contents were considered to be 150 mL of blood, and the remainder of the blood volume was considered to contribute to the total body residence time. The dynamic bladder model and the International Commission on Radiological Protection (ICRP) 30 gastrointestinal tract model were not used.

Dose Calculation for Basal Ganglia

TACs for the basal ganglia were determined from the PET scans by drawing a multiplane ROI over the putamen and then determining the maximum uptake within the ROI. The uptake concentration of the putamen was assumed to reflect the uptake concentration of the entire basal ganglia.

Because of the inherent limited spatial resolution of PET scanners, correcting for the partial-volume effect is necessary (*11*,*12*). The partial-volume correction was determined experimentally by comparing the activity in the punch biopsies of the putamen with the value measured by the scanner, using the methodology of Kessler et al. (*11*).

Residence times for the basal ganglia and brain were calculated, as described above, by trapezoidal integration of the partial-volume corrected data and then by analytic integration of the fit monoexponential curve.

S-factors necessary in the calculation of the radiation-absorbed dose for the basal ganglia are not currently available. Because the human testes are approximately the same size and shape as the human basal ganglia, the MIRDOSE3 S-factors for the testes were used. The self-dose to the basal ganglia was estimated by entering the residence time for the basal ganglia as the testes residence time in a separate run of MIRDOSE3. This provided an estimate of the radiation-absorbed dose from the decay of ^{18}F within the basal ganglia. The 0.511-MeV annihi-

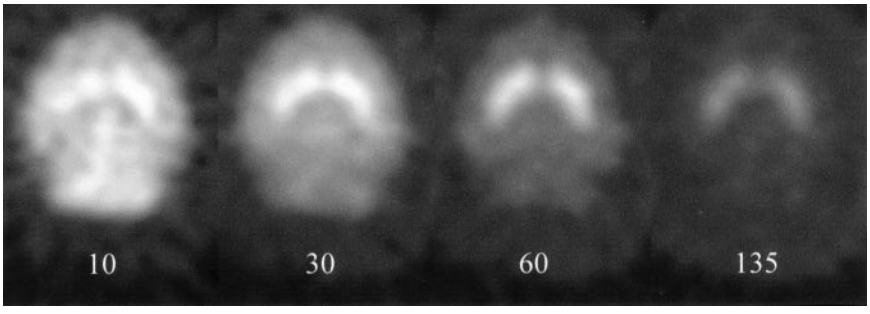

FIGURE 1. [^{18}F]FECNT images at indicated times (min) after injection. Putamen-to-background ratios are 1.1, 2.25, 3.59, and 2.74, respectively.

TABLE 1
Sample Calculation for Residence Time in Testes

Model	Time of sacrifice after injection (min)	Uptake*	Uptake (%) per organ†	Exponential fit to monkey data	Trapezoidal integration (uptake % min)	Residence time (h)‡
Sprague-Dawley rat	5	1.463	0.062		0.155	
data	30	1.289	0.055		1.462	
	60	1.055	0.045		1.495	
	120	0.563	0.024		2.064	
Rhesus monkey data	174	0.015	0.037	0.025	1.653	
	194	0.006	0.015	0.021	0.519	
	236	0.004	0.010	0.014	0.522	
	242	0.005	0.013	0.014	0.071	
	246	0.004	0.009	0.013	0.045	
	268	0.007	0.017	0.011	0.287	
	352	0.003	0.008	0.005	1.051	1.55×10^{-3}
Combined						1.78×10^{-3}

*Rat data, relative; monkey data, %ID/g.
†Rat data were scaled by factor of 0.0425. Monkey data were scaled to organ mass of 2.5 g.
‡Summation of trapezoidal integration up to 352 min gives 1.55×10^{-3} h; analytic integration of exponential fit to monkey data after 352 min gives 2.3×10^{-4} h, for total residence time of 1.78×10^{-3} h.

lation photons associated with the ^{18}F decay are assumed to contribute very little to the basal ganglia dose because their mean free path in brain tissue (taken to be the same as in water [~10 cm]) is much greater than the dimension (~2 cm) of the basal ganglia. The resulting dose from MIRDOSE3 is an underestimate of the self-dose to the basal ganglia, because the absorbed dose is averaged over the human testes mass of 35 g rather than the human basal ganglia mass of 26 g (*13*). Because the dose is primarily from positrons, it is corrected by scaling by the ratio of the testes to basal ganglion masses. The self-dose to the basal ganglia was then added to the total brain dose from all other organs, giving the estimated total dose to the basal ganglia.

RESULTS

From time of injection to time of killing, no adverse effects were observed during or after the administration of [^{18}F]FECNT in either the Sprague-Dawley rats or the rhesus monkeys. The two monkeys that were not killed were observed continuously for approximately an additional month and also showed no apparent adverse effects. All chemical doses were believed to be in tracer concentrations and well below the amount necessary to cause physiologic effects.

Table 2 contains the scaling factors used to match the rat data to the monkey data, the estimated organ clearance rates, and the estimated residence times for each organ. Uncertainty in the clearance parameter of the monoexponential curve that was fit to the monkey data is the greatest source of error associated with the residence time calculation for each organ. To estimate the magnitude of the error, the clearance parameter was purposefully made too large, and the residence times were recalculated. An amount equal to the SE of the parameter, as determined from the curve fit, was used to increase the parameter. The Sprague-Dawley rat data were then rescaled to match the new fit line, and the residence times

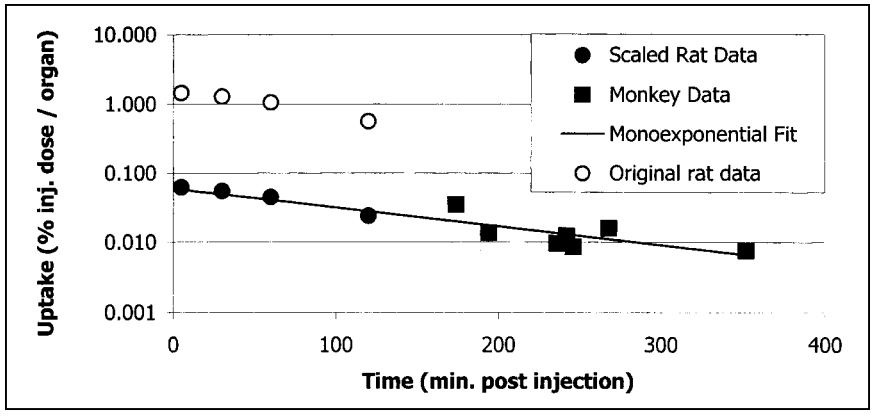

FIGURE 2. Graph of combined Sprague-Dawley rat and rhesus monkey data for testes. Original rat data (○) have been scaled (●) to match monkey data (■). Residence time is calculated by numeric integration of adjusted data points and analytic integration of fit after last data point.

TABLE 2
Residence Times

Organ	Scaling factor*	Clearance half-time (h)	Residence time (h)	Estimated error (%)
Basal ganglia	—	2.77	1.38×10^{-2}	30
Heart	1.10	1.12	9.03×10^{-3}	7
Lungs	2.00	1.04	2.84×10^{-2}	24
Liver	0.28	1.80	3.59×10^{-2}	15
Spleen	0.88	1.17	5.62×10^{-3}	10
Kidney	0.38	2.17	1.17×10^{-2}	16
Cortical bone	0.44	1.64	6.43×10^{-2}	13
Trabecular bone	0.44	1.64	6.43×10^{-2}	13
Muscle	0.62	1.67	4.69×10^{-1}	8
Testes	0.04	1.97	1.73×10^{-3}	14
Blood	0.65	1.64	1.45×10^{-1}	5
Brain	—	1.00	7.95×10^{-2}	20
Total body†	—	—	1.73×10^{0}	2.6

*Empirically derived factor used to match rat and monkey data.
†Basal ganglia residence time was not included in calculation of total body residence time.

were recalculated. This second residence time was compared with the original residence time to estimate the error in the dose calculation. Error in the total body residence time was calculated by propagating errors for the separate organ residence times.

An average measured contrast-recovery coefficient of 0.40 was used to correct the monkey putamen TACs for the partial-volume effect. Figure 3 illustrates how the partial- volume-effect correction altered the basal ganglia data. Also in Figure 3 is an averaged TAC for the cerebellum of both monkeys, to illustrate the selectivity of [^{18}F]FECNT for the dopamine-rich basal ganglia. Radiation-absorbed doses from the MIRDOSE3 program are presented in Table 3.

DISCUSSION

Ideally, rhesus monkey data would have been used in place of the Sprague-Dawley rat data. But killing enough rhesus monkeys to cover the first 2 h after injection was not feasible. Inclusion of the Sprague-Dawley rat data under the provisions detailed by Kirschner et al. (*8*) allows an estimation of the shape of the TACs before the earliest monkey biodistribution data. It is assumed that the combined rat and rhesus data result in a better estimate of the residence times for the organs. Extrapolating the rhesus monkey data alone back to the injection time and recalculating gives a smaller dose. The combination of the Sprague-Dawley rat data and the rhesus monkey data does not take into consideration any time-dependent differences between the metabolic rates of rats and monkeys. The purpose of this study was to determine a conservative estimate of the radiation-absorbed dose to humans by using all available data.

The average putamen TAC determined by PET in the rhesus monkey, corrected for partial-volume effect and decay, is shown in Figure 3. Had the partial-volume effect not been considered in the computation of the residence time, the dose to the basal ganglia would have been underestimated by at least a factor of 2.

The dosimetry of commonly used ligands necessary to study the dopamine system, such as [^{11}C]raclopride (*14*,*15*) and [^{123}I]fluoropropyl-2β-carbomethoxy-3β-[4-iodophenyl] tropane (*16*), can be compared with the dosimetry results of [^{18}F]FECNT (Table 4). The dosimetry of [^{18}F]FECNT is similar to that of these other dopamine transporter ligands used to study the dopamine system.

In this study, no tracer excretion was considered; this will have the effect of overestimating the dose to most body organs but possibly underestimating the dose to the bladder or intestines. Although not specifically addressed here, increasing both the bladder volume (*17*) and fre-

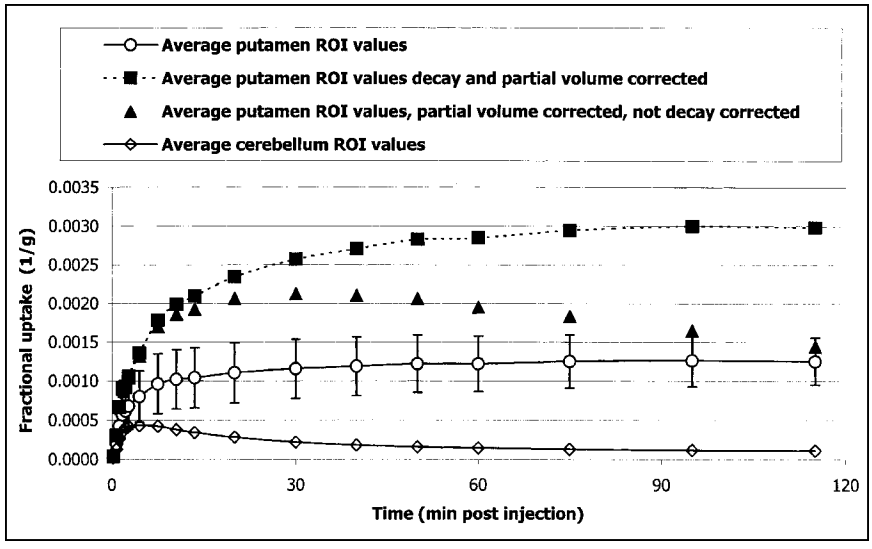

FIGURE 3. Average (n = 3) TACs for [^{18}F]FECNT in basal ganglia of rhesus monkeys. Comparison of partial-volume–corrected, nondecay-corrected putamen (▲) and cerebellum (◇) indicates specific uptake of [^{18}F]FECNT in dopamine-rich areas. Curve represented by triangles was used to calculate basal ganglia residence time.

quency of voiding (*18*) may reduce the dose to the urinary bladder wall in humans. Additionally, urine and feces should be collected, and the dynamic bladder model and the ICRP 30 gastrointestinal tract model should be used in further dosimetric work with [^{18}F]FECNT on humans, to more accurately estimate the dosimetry after human studies begin.

CONCLUSION

The biodistribution of [^{18}F]FECNT in rats and monkeys was measured, and radiation dosimetry in humans was estimated. A 185-MBq (5-mCi) injection of [^{18}F]FECNT results in an effective dose of 3 mSv (0.3 rem) and an estimated dose to the target region, the basal ganglia, of 19.4 mGy (1.93 rad). The organs and regions receiving the next highest doses are the heart wall (7.7 mGy [0.77 rad]), small intestine (3.3 mGy [0.33 rad]), and pancreas (3.3 mGy [0.33 rad]). Although further dosimetry work should be performed on humans as [^{18}F]FECNT becomes used in the clinic, these estimates can be used to plan the first human studies.

TABLE 3
Estimated Radiation Adsorbed Doses from [^{18}F]FECNT

Organ	MGy/MBq	rad/mCi
Basal ganglia	1.05×10^{-1}	3.87×10^{-1}
Heart wall	4.17×10^{-2}	1.54×10^{-1}
Small intestine	1.79×10^{-2}	6.61×10^{-2}
Pancreas	1.77×10^{-2}	6.53×10^{-2}
Uterus	1.77×10^{-2}	6.55×10^{-2}
Thymus	1.75×10^{-2}	6.47×10^{-2}
Upper large intestine wall	1.74×10^{-2}	6.46×10^{-2}
Ovaries	1.74×10^{-2}	6.43×10^{-2}
Brain	1.73×10^{-2}	6.41×10^{-2}
Lower large intestine wall	1.70×10^{-2}	6.29×10^{-2}
Stomach	1.69×10^{-2}	6.26×10^{-2}
Gallbladder wall	1.68×10^{-2}	6.23×10^{-2}
Urinary bladder wall	1.67×10^{-2}	6.20×10^{-2}
Adrenals	1.65×10^{-2}	6.12×10^{-2}
Red marrow	1.61×10^{-2}	5.96×10^{-2}
Thyroid	1.49×10^{-2}	5.53×10^{-2}
Kidneys	1.45×10^{-2}	5.36×10^{-2}
Bone surfaces	1.40×10^{-2}	5.17×10^{-2}
Breasts	1.38×10^{-2}	5.10×10^{-2}
Testes	1.38×10^{-2}	5.11×10^{-1}
Spleen	1.30×10^{-2}	4.82×10^{-2}
Lungs	1.25×10^{-2}	4.61×10^{-2}
Total body	1.24×10^{-2}	4.58×10^{-2}
Skin	1.19×10^{-2}	4.41×10^{-2}
Liver	1.04×10^{-2}	3.84×10^{-2}
Muscle	9.72×10^{-2}	3.60×10^{-2}
Effective dose equivalent*	1.75×10^{-2} mSv/MBq	6.46×10^{-2} rem/mCi
Effective dose*	1.58×10^{-2} mSv/MBq	5.84×10^{-2} rem/mCi

*Dose to basal ganglia was not included in estimate of effective dose and effective dose equivalent.

TABLE 4
Comparison of Dosimetry (mGy/MBq) of Ligands Used to Study Dopamine System

Organ	[^{18}F]FECNT	[^{11}C]Raclopride*	[^{123}I]FP-CIT†
Gallbladder wall	1.70×10^{-2}	6.1×10^{-2}	2.57×10^{-2}
Bladder wall	1.70×10^{-2}	1.7×10^{-2}	2.57×10^{-2}
Liver	1.03×10^{-2}	3.2×10^{-2}	2.85×10^{-2}
Small intestine	1.81×10^{-2}	1.6×10^{-2}	2.07×10^{-2}
Kidney	1.43×10^{-2}	9.0×10^{-3}	1.12×10^{-2}
Lungs	1.24×10^{-2}	4.25×10^{-2}	
Basal ganglia	9.78×10^{-2}	2.3×10^{-1}	
Effective dose Equivalent (mSv/MBq)	1.75×10^{-2}		2.44×10^{-2}
(mSv/MBq)	1.58×10^{-2}	1.0×10^{-2}	2.38×10^{-2}

*From Herskovitch et al. (*15*).
†From Booij et al. (*16*).

ACKNOWLEDGMENTS

The authors are grateful for the technical contributions of Delicia B. Votaw and Vernon M. Camp and to Carolyn K. Malcolm for assistance in preparing the manuscript.

REFERENCES

1. Carroll FI, Lewin AH, Boja JW, Kuhar MJ. Cocaine receptor: biochemical characterization and structure-activity relationships of cocaine analogues at the dopamine transporter. *J Med Chem.* 1992;35:969–981.
2. Volkow ND, Wang GJ, Fischman MW, et al. Relationship between subjective effects of cocaine and dopamine transporter occupancy. *Nature.* 1997;386:827–830.
3. Kaufmane MJ, Madras BK. Severe depletion of cocaine recognition sites associated with the dopamine transporter in Parkinson's diseased striatum. *Synapse.* 1991;49:43–49.
4. Goodman MM, Kabalka GW, Kung MP, Kung HF, Meyer MA. Synthesis of [^{18}F]-N-3-fluoropropyl-2=DF-carbomethoxy-3=DF-4-chlorophenyl)tropane: a high affinity neuroligand to map dopamine uptake sites by PET. *J Label Cmpd Radiopharm.* 1994;34:488–490.
5. Goodman MM, Kilts CD, Keil R, et al. ^{18}F-labeled FECNT: a selective radioligand for PET imaging of brain dopamine transporters. *Nucl Med Biol.* 2000;27:1–12.
6. Goodman MM, Keil R, Shoup TM, et al. Fluorine-18-FPCT: a PET radiotracer for imaging dopamine transporters. *J Nucl Med.* 1997;38:119–126.
7. Zamora PO, Eshima D, Graham D, Shattuck L, Rhodes BA. Biological distribution of ^{99m}Tc-labeled YIGSR and IKVAV laminin peptides in rodents: ^{99m}Tc-IKVAV peptide localizes to the lung. *Biochim Biophys Acta.* 1993;1182:197–204.
8. Kirschner AS, Ice RD, Beierwaltes WH. Radiation dosimetry of ^{131}I-19-iodocholesterol. *J Nucl Med.* 1973;14:713–717.
9. Kirschner A, Ice R, Beierwaltes W. Letters to the editor. *J Nucl Med.* 1975;16:248–249.
10. Stabin MG. MIRDOSE: personal computer software for internal dose assessment in nuclear medicine. *J Nucl Med.* 1996;37:538–546.
11. Kessler RM, Ellis JR Jr, Eden M. Analysis of emission tomographic scan data: limitations imposed by resolution and background. *J Comput Assist Tomogr.* 1984;8:514–522.
12. Hatazawa J, Hatano K, Ishiwata K, et al. Measurement of D2 dopamine receptor-specific carbon-11-YM-09151-2 binding in the canine brain by PET: importance of partial volume correction. *J Nucl Med.* 1991;32:713–718.
13. Blinkov SM, Glezer II. *The Human Brain in Figures and Tables: a Quantitative Handbook.* New York, NY: Basic Books, Inc. [Plenum Press]; 1968:166.
14. Farde L, Halldin C, Stone-Elander S, Sedvall G. PET analysis of human dopa-

mine receptor subtypes using ^{11}C-SCH 23390 and ^{11}C-raclopride. *Psychopharmacology.* 1987;92:278–284.
15. Herscovitch P, Schmall B, Doudet D, Carson R, Eckelman W. Biodistribution and radiation dose estimates for [11-C]raclopride [abstract]. *J Nucl Med.* 1997; 5(suppl):224.
16. Booij J, Busemann Sokole E, Stabin MG, Janssen AGM, de Bruin K, van Royen EA. Human biodistribution and dosimetry of [^{123}I]FP-CIT: a potent radioligand for imaging of dopamine transporters [published erratum appears in *Eur J Nucl Med.* 1998;25:458]. *Eur J Nucl Med.* 1998;25:24–30.
17. Dowd MT, Chen CT, Wendel MJ, Faulhaber PJ, Cooper MD. Radiation dose to the bladder wall from 2-[^{18}F]fluoro-2-deoxy-D-glucose in adult humans. *J Nucl Med.* 1991;32:707–712.
18. Votaw JR, Ansari MS, Mason NS, et al. Dosimetry of iodine-123-epidepride: a dopamine D2 receptor ligand. *J Nucl Med.* 1995;36:1316–1321.